Investigation of Physically and Chemically Ionic Liquid Confinement in Nanoporous Materials by a Combination of SANS, Contrast-Matching SANS, XRD and Nitrogen Adsorption

To cite this article: G E Romanos *et al* 2012 *J. Phys.: Conf. Ser.* **340** 012087

Investigation of Physically and Chemically Ionic Liquid Confinement in Nanoporous Materials by a Combination of SANS, Contrast-Matching SANS, XRD and Nitrogen Adsorption

G E Romanos[1*], K L Stefanopoulos[1], O C Vangeli[1], K Mergia[2], K G Beltsios[3], N K Kanellopoulos[1] and D Lairez[4]

[1] Institute of Physical Chemistry and [2] Institute of Nuclear Technology and Radiation Protection, NCSR "Demokritos", Ag. Paraskevi Attikis, 15310, Greece
[3] Department of Materials Science and Engineering, University of Ioannina, 45110, Greece
[4] Léon Brillouin, CEA/CNRS UMR 12, CEA-Saclay, 91191 Gif-sur-Yvette cedex, France

[*]groman@chem.demokritos.gr

Abstract. In the present study, [bmim][PF_6] ionic liquid (IL) was introduced into the pores of two ordered mesoporous silicas (MCM-41 and SBA-15) having different pore sizes by means of two different processes: a) with physical imbibition from a methanol solution under high vacuum and b) by chemically immobilising the IL with silanisation of the pore surface followed by reaction with butyl-methyl imidazolium chloride and anion exchange with PF_6, the process termed as the "grafting to" method. Both the extent of IL entrapment and the structural properties of the IL phase under confinement were investigated by SANS, contrast-matching SANS, XRD and nitrogen adsorption measurements. The results show that the pores of chemically prepared samples are not totally filled by IL and also suggest for ordering of the silylated IL phase. On the other hand, the physically prepared samples are almost or totally filled with IL whereas no evidence for ordering of the confined IL phase was observed.

1. Introduction

Room-temperature ionic liquids (ILs), an increasingly important set of electrolytes, have received much attention due to their unique characteristics: low vapour pressure, thermal stability, non-flammability, chemical tuneability and good electrolytic and solvation properties. Furthermore the incorporation of ILs into the pore structure of advanced porous materials (carbon nanotubes [1], ordered mesoporous silicas) for the formation of supported ionic liquid phase systems (SILPs), or into the nanopores of the separating layer of asymmetric membranes (carbon, ceramic, polymeric) is of key importance and consists the only way to overcome major drawbacks of ILs such as, their high viscosity, slow gas diffusivity and high price, making feasible their large scale application as solvents, catalyst dispersion agents and absorbents in the fields of organic synthesis, heterogeneous catalysis and gas separation. The development of well-stabilised thin IL films on the high pore surface area (1000 m^2/g) of advanced porous materials may considerably reduce the quantity of IL that is necessary for a certain scale of application and in parallel makes it possible to exploit all of the mass of the incorporated IL, since viscosity and diffusion effects may be diminished in such ultra thin layers. In this regard the interaction of ILs with solid surfaces [2-4] and, both their state and morphology after incorporation into the pore structure are issues that deserve further investigation.

For example if the IL phase, under extreme confinement into the nanopores, is crystallised then the benefits derived from the thin film formation and the high surface area, which is available for reaction or adsorption, are counterbalanced by the slower diffusion rates holding for the solid phase compared to the liquid one. Moreover, if the pore structure of the supporting material is blocked due to extended IL deposition onto the pore mouths or if the entire pore structure is completely filled with the liquid IL phase, then all the potential benefits of SILPs are taken out. Finally, it is often the case that high temperatures and differential pressures are required in some catalytic or gas separation processes, which despite the low vapour pressure of ILs, could lead to their significant evaporation or displacement out of the pore structure. In this regard it is preferable to further stabilise ILs through the formation of a chemical bond, rather than rely the stability solely on the physical and electrostatic interaction between the IL's ions and the pore walls. The chemical attachment of the cation or the anion on to the pore wall may, in addition, lead to a preferable orientation of the IL's layers towards the core of the pore, which accommodates the reactants or the adsorbates. This orientation may be favorable when selective penetration from a gas or liquid mixture is required i.e. exploiting the hydrophilic or hydrophobic character of the ions and can bring the advance of higher diffusion rates, especially for IL membranes, where the gas transport is described as a sequential process of complexation-decomplexation of the gas molecule with the IL's ions, usually the anions. For the aforementioned reasons, it is essential to develop and examine methods that are sensitive to the bulk of the pore structure and not to the pore opening as the widely used N_2 porosimetry and the advanced microscopy techniques.

Small-angle scattering of neutrons or x-rays (SANS or SAXS) [5-8], contrast-variation or contrast-matching SANS [9-13] and adsorption in conjunction with neutron (x-ray) diffraction or SANS (SAXS) [14-20] have been proved to be essential tools for elucidating the microstructure of nanoporous materials and the properties of confined phases within the pores. Moreover, combination of SANS and 3D stochastic reconstruction methods is also a powerful tool for visualising the evolution of the adsorption mechanism and show how sorption alters the pore space characteristics of the material [21-22]. SANS has the advantage over the conventional gas adsorption methods that it can provide information for the bulk of the structure, including pores inaccessible to gas molecules, such as closed pores. Previous SANS experiments on IL in cyclohexane oil emulsions demonstrated the formation of surfactant-stabilised dispersed nanodroplets with IL cores [23]. Recently, voltage-clamp measurements through single conical nanopore obtained by chemical etching of a single ion track in polyimide film were reported [24]. The results showed that the origin of the pink noise of the ionic current could be ascribed to a cooperative effect on ions motion in confined geometry. Furthermore, silica based ordered mesoporous materials like MCM-41 and SBA-15 consist of a two-dimensional hexagonal arrangement of cylindrical mesopores of uniform size (*P6mm* space group). They are materials exhibiting Bragg peaks in the small-angle regime due to the regular packing of the cylindrical pores and they are considered as model systems for both adsorption studies and mesopore size determination. They are synthesised by using micellar aggregates of surfactans (MCM-41) [25] or amphiphilic block copolymers (SBA-15) [26] as structure-directing template and their pore size can be tailored by the choice of the amphiphile.

We are now proposing the potentiality of SANS and contrast-matching SANS for studying both the extent of pore filling and the organisation of confined [bmim][PF_6] IL in the nanopores of two ordered nanoporous materials (MCM-41 and SBA-15) with different pore sizes. The IL was introduced a) by physical imbibition under vacuum and b) by the "grafting to" method involving chemical immobilisation by means of silanisation of the pore surface followed by reaction with butyl-methyl imidazolium chloride and anion exchange with PF_6. In addition, N_2 adsorption isotherms at 77 K and x-ray diffraction (XRD) measurements have been carried out.

2. Experimental

2.1. Materials and chemicals

The materials MCM-41 and SBA-15 (named as MCM and SBA) were provided by Sigma-Aldrich® and Claytec Inc. respectively. Solvents were used as purchased without 'further drying'. Diethyl ether (puriss, Reag ACS, Aldrich), chloroform (GC, Aldrich), acetonitrile (GC, Aldrich), methanol (99.8%, Aldrich). Reaction reagents were used as purchased without 'further purification'. Chlorobutane (99%, Fluka), 1-methylimidazole (99% redistilled, Aldrich), (chloropropyl)-trimethoxysilane (96%, Aldrich), sodium hexafluorophoshate (98%, Aldrich). The [bmim][PF_6] IL was prepared in a similar way previously reported [27-28] and its purity was confirmed by NMR.

2.2. Pore filling procedures

The pore filling of the samples with IL was achieved by physical imbibition of [bmim][PF_6] from its methanol solution under vacuum (prepared samples named as MCM_PHYS and SBA_PHYS) and by chemical grafting of the IL under reflux conditions (prepared samples named as MCM_SILP and SBA_SILP).

2.2.1. *Physical imbibition.* A vacuum assisted physical imbibition method was involved in order to facilitate the pore filling process. More specific crimp top-flat bottom headspace vials of 20 ml were appropriately modified to permit the application of high vacuum (10^{-3} mbar) into their internal space. The modification consisted on the welding of the common port of a high vacuum three-way glass valve (ACE 8145-06 three-way stopcock) on the sidewall of the vials close to their bevelled neck. About 200 mg of the SBA and MCM powders, having an absolute pore volume of 0.19 and 0.25 cm^3 respectively, were placed on the bottom of the vials together with a stirring magnet and the vials were tightly sealed by means of crimp caps and PTFE/black butyl molded septa. The three-way valve was then turned to the vacuum working port and the vials were in parallel heated to 200 ^oC to allow the removal of the adsorbed water phase from the solid surface. After 24 h, the temperature was decreased to 60 ^oC the valve was turned to the off position and a binary mixture of [bmim][PF_6] and methanol (v/v) 1:1 (5 ml solution) was injected on the powder by means of a glass syringe that perforated the septa. The powder suspension was left for another 24 h under stirring to assist the infiltration of the IL solution into the pores. In order to break the vacuum and avoid the direct contact with the air moisture the three-way valve was turned to the gas working port permitting the introduction of 1 bar of argon into the vial. After several hours without stirring the supernatant aliquot was suctioned by means of the glass syringe and replaced with pure methanol. The washing with methanol was repeated 5 times to remove most of the excess IL before proceeding with the solvent evaporation (rota-vapour) to yield the IL impregnated solid powder.

2.2.2. *Chemical-"grafting to" method.* A 200 mg portion of MCM and SBA was dried at 423 K under a vacuum for 1 h. To the solid support, a solution of (3-chloropropyl)-trimethoxysilane (2.5 mL, 13.5 mmol) in $CHCl_3$ (10 mL) was added (67.5 mmol silylant/g sample) and the mixture was refluxed under stirring and N_2 atmosphere for 48 h. After filtration, the hybrid material was washed consequently by refluxing in pentane (30 mL), CH_3CN (30 mL), and diethyl ether (30 mL) followed by drying for 1 h at 343 K. Following, the chloropropylated hybrid material was reacted with 1-methylimidazole (5 mL) under N_2 atmosphere at 358 K and remained under rotation for 48 h. The reaction mixture was filtered and the hybrid material was refluxed with diethyl ether (30 mL) for 30 min and then filtered and dried at 343 K for 1 h. To the synthesised [spmim][Cl] hybrid material a solution of $NaPF_6$ (68 mg, 0.4 mmol) in ethanol (6 mL) was added under N_2 atmosphere and the mixture remained under stirring for 5 d at room temperature. Reaction progress for the ion exchange step was monitored with the $AgNO_3$ test, which was positive from the first 24 h from reaction onset. The hybrid material was consequently filtered, washed by refluxing with methanol (30 mL) for 30 min, filtered, and dried in a vacuum for 1 h.

2.3. Instrumentation

The nitrogen adsorption isotherms have been performed volumetrically at 77 K on an Autosorb-1 MP gas analyzer, (Quantachrome instruments). The samples were initially outgassed at 160 ^{o}C for 12 h, under high vacuum ($<10^{-6}$ mbar). Pore size distributions, according to BJH [29] and non-local density function theory (NLDFT) [30-31] methods, have been derived from the commercial software AS1win (provided by Quantachrome instruments).

The XRD measurements were performed on a D8 Advance Bruker diffractometer using Cu-Kα radiation and parallel beam stemming from a Göbel Mirror. The measurements were carried out in a 2θ region between 15 and 55^{0} corresponding to a Q range varying from 10.7 to 37.7 nm^{-1} .

The SANS measurements were carried out at the PACE spectrometer (LLB, Saclay, France) in a Q-range varying from 0.035 to 3 nm^{-1} corresponding to two sample-detector distances (4.56 m and 1.06 m respectively). The samples were in powdered form and were mounted in a 1 mm thick sealed quartz container (provided by Hellma). For the contrast-matching SANS measurements, they were immersed in an appropriate H_2O/D_2O mixture. The “wet” samples, MCM_w, MCM_PHYS_w, MCM_SILP_w, SBA_w, SBA_PHYS_w and SBA_SILP_w were allowed for 4 h to come to equilibrium before measurement [32]. Absolute values for the intensity, $I(Q)$, were obtained by correcting the raw data for sample transmission, scattering of the empty cell and instrumental background; as a final step, the data were calibrated against a water standard [33]. All corrections were treated by using the software PASINET (for a detailed procedure of data treatment, see ref. 33).

3. Results and discussion

3.1. N_2 adsorption isotherms

The figures 1a and 1b illustrate the N_2 adsorption isotherms at 77 K of both set of samples (MCM, MCM_SILP, MCM_PHYS) and (SBA, SBA_SILP, SBA_PHYS) respectively. Further, the structural characteristics of the samples are reported at table 1. The specific surface area, S, was determined by the BET method [34], while the total pore volume, V_p, was derived from the amount adsorbed at relative pressure, $p/p_0 \approx 0.97$. Finally, pore size distributions were deduced based on both BJH (Table 1) and NLDFT methods (insets of figures 1a and 1b and table 1).

Table 1. Structural parameters of the samples obtained by nitrogen adsorption and SANS measurements*.

Sample	S (m^2/g)	V_p (cm^3/g)	R_p^{BJH} (nm)	R_p^{NLDFT} (nm)	a_0 (nm)
MCM	1070	1.27	1.5	2.1	4.4
MCM_SILP	320	0.42	1.9	2.5	4.4
MCM_PHYS	110	0.33			4.4
SBA	700	0.93	2.8	3.7	10.3
SBA_SILP	480	0.67	3.0	3.8	10.3
SBA_PHYS	17	0.02			10.3

*Abbreviations: S: Specific surface area, V_p: pore volume,: R_p^{BJH} pore radius evaluated by the BJH method, R_p^{NLDFT}: pore radius calculated by the NLDFT method, a_0: lattice parameter estimated from the interplanar d_{10} spacing of SANS data ($a_0 = 2d_{10} / \sqrt{3}$).

The isotherms of the pristine samples (MCM and SBA respectively, figures 1a and 1b) are of type IV, according to the IUPAC classification [35]. Both samples exhibit a hysteresis loop (type H1 by IUPAC classification) corresponding to capillary condensation and evaporation on open cylindrical pores at both ends. The step associated with capillary condensation in the cylindrical mesopores commences at $p/p_0 \approx 0.4$ for the MCM sample whereas for the SBA the correspondent relative pressure is about 0.6. The fact that capillary condensation occurs at a higher relative pressure in the case of SBA compared to the MCM is related to its larger pore size. The upturn of the isotherms from both pristine samples at pressures close to the vapour pressure is attributed to large mesopores, formed between the silica particles.

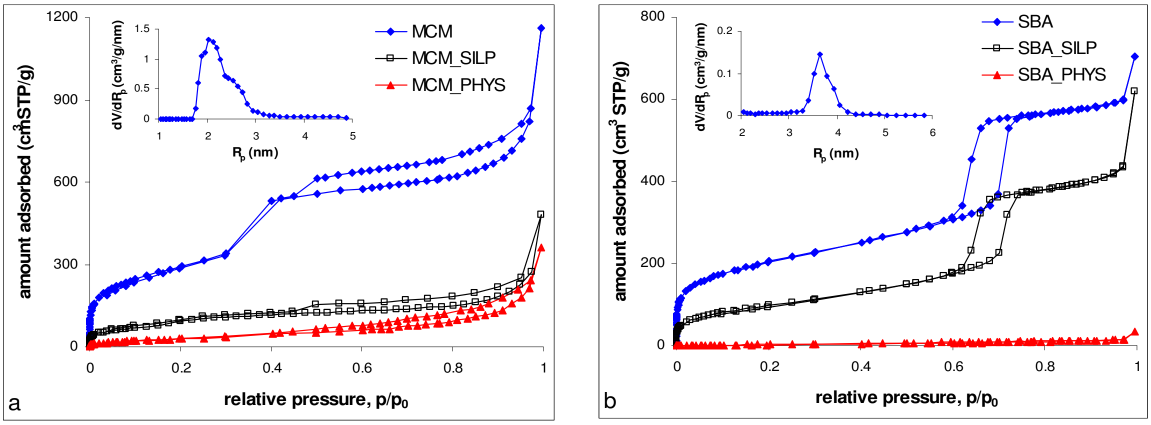

Figure 1. Nitrogen adsorption isotherms at 77 K of (a) MCM, MCM_SILP, MCM_PHYS and (b) SBA, SBA_SILP, SBA_PHYS samples. (Insets: pore size distributions of pristine (a) MCM and (b) SBA samples according to NLDFT method).

On the other hand, in the case of the physically-loaded sample (SBA_PHYS), the amount adsorbed is almost zero (figure 1b). Since N_2 is not dissolved in the particular IL phase the result indicates a total absence of accessibility of N_2 molecules to the pore network, suggesting that the pores are totally filled with IL or the pore mouths are completely blocked rendering the bulk of the pore inaccessible for adsorption. Obviously, pore size distribution is not possible to be extracted. Further, the adsorption isotherm of the MCM_PHYS sample (figure 1a), does not provide reliable information on the pore blocking extent. In particular, the isotherm nearly coincides with that of a non-porous reference silica sample [36], suggesting that the measured adsorbed volume can be attributed to the interparticle space. This argument is also supported by the fact that no reliable pore size distribution can be deduced by either BJH or NLDFT methods. However, as it will be further discussed, the SANS results imply that the pore "core" of the MCM_PHYS sample is empty despite the fact that the MCM pore size is smaller compared to the SBA one (table 1).

The N_2 isotherms of the SILP samples indicate that there is still significant pore space which remains open after grafting the IL molecule. Indeed, the maximum loading that can be achieved with the "grafting to" method is limited to the formation of a monolayer of the silanised IL on to the pore surface. Concerning the SBA_SILP sample, it is certain that the size of the silanised IL, silyl-propyl methyl-imidazolium hexafluorophosphate [spmim][PF_6], is not large enough to result in the effective blockage of the accessibility to the bulk of the pore (3.7 nm). Moreover, the "grafting to" method led solely to a significant reduction of the pore volume but not to alteration of the pore size (table 1). One may then conclude that the grafted IL molecules do not form a dense monolayer on the pore surface (see figure 2). This is something expected due to the sparse population of the surface silanol groups [27] that serve as the anchoring agents of the silyl part of the silanised IL. In this regard, there are still significant areas along the parallel cylindrical pores that are unaffected and where capillary condensation of N_2 occurs at relative pressures identical to these observed for the untreated samples.

Interesting to note is that the pore volume reduction is much more enhanced in the MCM_SILP compared to the SBA_SILP sample. In addition, there is a remarkable shift of the mean pore size to larger values (table 1). The difference in the pore volume reduction can be attributed to the different extent of IL loading, which in the case of the SILP samples is strongly related to the initial population of the silanol groups on the surface of the ordered mesostructured silicas. In this regard, we can state that the silanol population of MCM_SILP is much higher compared to this of the SBA_SILP.

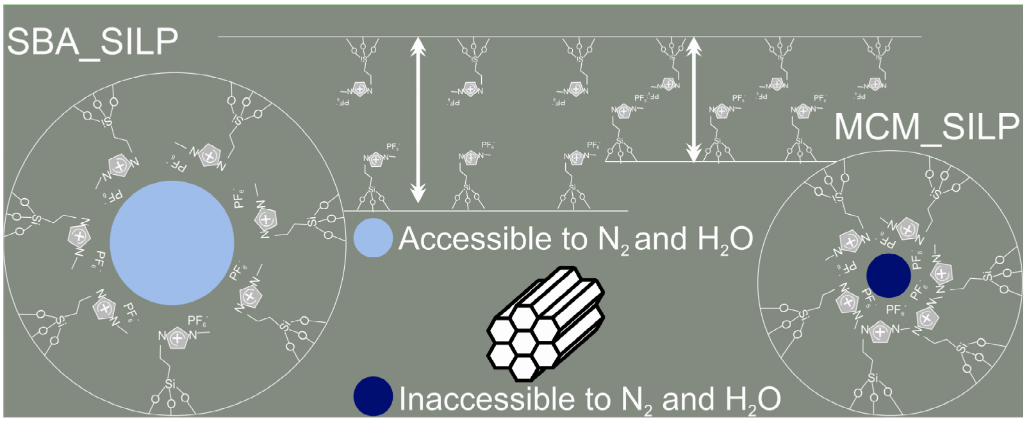

Figure 2. Schematic drawing of the pore loaded with IL in MCM_SILP and SBA_SILP samples according to the “grafting to” method (see text for details).

However, the enhanced pore loading itself, cannot reasonably explain the significant shift of the pore size. This effect can be rather attributed to the complete blocking of a small portion of the MCM_SILP’s nanopores (the smaller ones) by the [spmim][PF_6] molecules protruding from the pore walls (figure 2). The size of the [bmim][PF_6] has been recently calculated at 0.9 nm [37]. As a result, this argument seems quite reasonable by taking into account the silane part of the silylated IL [spmim][PF_6] and the space occupied by the surface hydroxyls, a size corresponding to approximately 1.3-1.5 nm for the grafted IL. Thus the ratio between the MCM’s mean pore radius (2.1 nm) and the silylated IL’s molecular size (1.5 nm) is close to unity and in this respect, a small negative deviation of some of the MCM’s pores from the average size can lead to their complete blockage by the grafted IL. The complete blockage of a fraction MCM’s pores is further evidenced by the comparison between the incoherent backgrounds of the contrast-matching SANS measurements.

3.2. XRD measurements

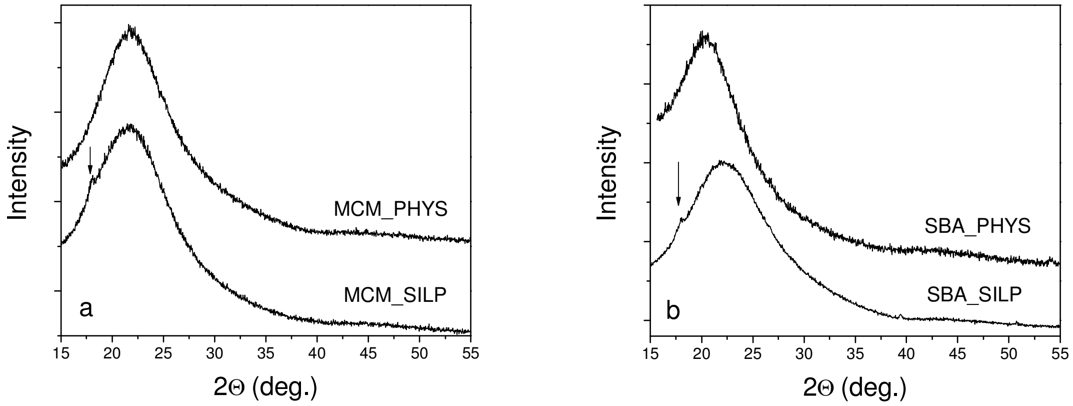

Figure 3. X-ray patterns of physically and chemically IL confinement on (a) MCM-41 and (b) SBA-15.

Figure 3 presents the diffraction spectra from all IL-loaded samples. In all cases, the broad reflection located about 22^0 is due to silica. Both SILP samples (MCM_SILP and SBA_SILP) show a diffraction peak appearing around 18^0 revealing ordering of the grafted silylated IL molecules. On the other hand, this Bragg peak is not observed for the samples loaded with IL via physical imbibition. A first remark is that the interaction of [bmim][PF_6] with the silica pore walls does not affect its ordering. This is in contrast with a case previously studied [38], concerning the interaction of the same IL with graphitic pore walls (carbon nanotubes). In a previous study [28], a degree of ordering was also observed on SILP samples developed on MCM-41 supports of various pore sizes. Based on current and previous XRD results [28] we can conclude that the extent of ordering cannot be directly related to the surface area, the pore volume and the pore size of the support but rather to the different degree of the IL loading because of the constriction effects.

3.3. *SANS and contrast-matching SANS*

Figure 4a (including the inset) shows the SANS curves from the dry pristine (MCM) and IL-loaded (MCM_SILP and MCM_PHYS) samples respectively. The hexagonal network of all samples produces one intense peak (10) and one weak (11). The high-order peaks are not observed because they are outside of the experimental *Q* window. In addition, the intensity of Bragg peaks for the samples treated with IL is decreased. In the case of the pristine SBA sample, except for the strong (10) reflection, the overlapping (11), (20) and the faint (21) Bragg peaks are visible.

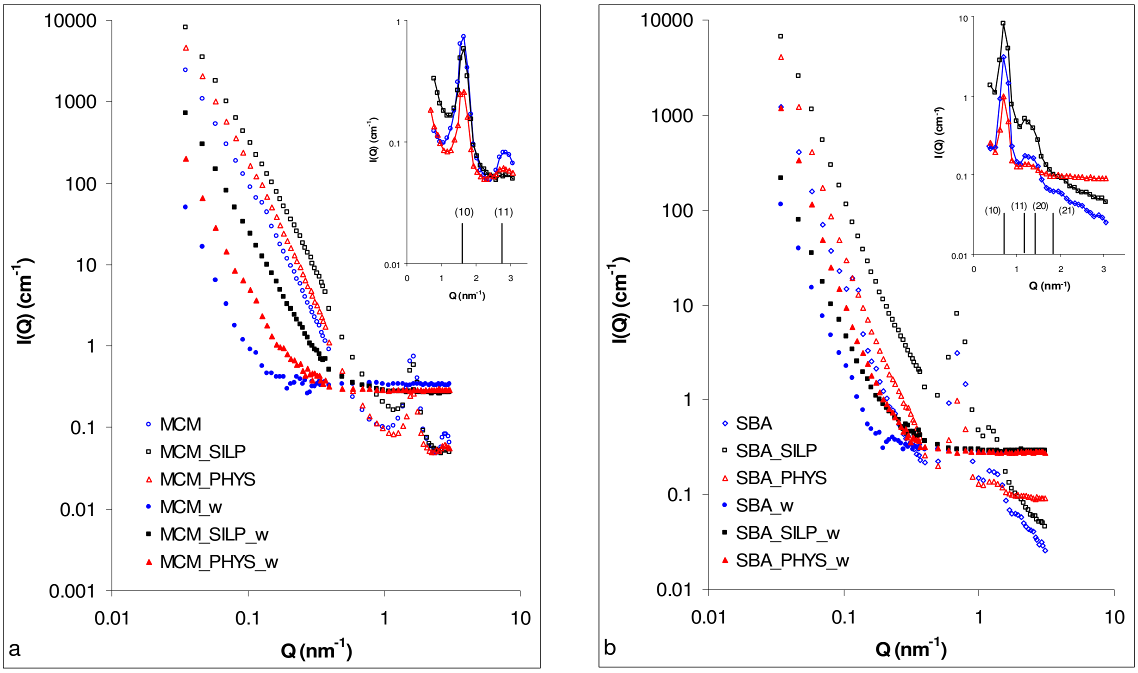

Figure 4. SANS and silica contrast-matching SANS curves from pristine and IL loaded (a) MCM and (b) SBA samples. (Insets: high-*Q* region spectral details of the pristine and IL loaded (a) MCM and (b) SBA samples; lines have been added as a guide to the eye for the peak positions; peak positions are also indicated by vertical lines).

On the other hand, the scattering from the SBA_PHYS sample becomes flat for $Q>1.6$ nm^{-1}, mainly due to the incoherent background arising from the hydrogen nuclei contained in the IL; this results in very weak (11) and (20) reflections and the absence of the (21) peak (figure 4b, including the inset). The presence of the incoherent background suggests that a larger amount of IL is confined on the pores via physical imbibition compared to the amount of IL confined by the "grafting to" method. This finding is in agreement with the N_2 adsorption measurements as discussed previously. Another observation is that the intensity of all Bragg peaks for the samples treated with IL, except for the case of SBA_SILP sample, is decreased. As it will be further discussed, this intensity increase implies a small IL loading into the pore space. The calculated values of the lattice parameter, a_0, are given at table 1. The fact that the lattice parameter for all samples (pristine and IL loaded respectively) remains unchanged implies a rather rigid solid matrix that does not alter upon filling with IL either physically or chemically.

In the low-Q region ($0.03<Q$ (nm^{-1})$<\sim 0.3$) the intensity follows a power law ($I(Q) \sim Q^{-a}$). According to the SANS theory, when $a=4$, the intensity decreases asymptotically as Q^{-4} following the so-called *Porod's law* [39]. In our case, the observed gradients, especially for the SBA samples, are close to Porod scattering, indicating a contribution from objects considerably larger than the cylindrical mesopores. In specific, it is normally observed in the tail of a SANS curve when $Qd>4$, where d is the size of the scattering object. Following this argument the size of such objects is >100 nm and can therefore be ascribed to intergrain interfacial scattering, as has also been observed in other studies [40-42]. The specific surface areas for pristine samples derived from the absolute intensities and the Porod function have values less than 2 m^2/g, also in agreement with previous studies [43]. These areas are far smaller than the correspondent BET surface areas (table 1) verifying that the scattering is indeed from the outer surfaces of the particles. Another interesting observation is an increase in intensity for all IL-loaded samples compared to the pristine ones. This behaviour can be attributed to the increase in the average contrast due to the fact that the intergrain space is filled with IL [44], also indicating that apart from the pore surface the external surface of the material is also covered by the IL phase.

SANS can be proved to be a powerful, if not a unique, technique for investigating whether the IL has been partially or completely filled within the pores of ordered mesoporous materials. This is one of the advantages of the SANS technique over the conventional gas adsorption methods because neutrons can also "see" pores which are inaccessible to gas molecules (such as closed pores). For instance, IL could have been dispersed around the pore surface preventing, thus, the access to N_2 molecules. According to the scattering theory, for a two-phase system (for instance, SiO_2-empty pore and SiO_2-IL), the intensities of the Bragg reflections are related to the square of the contrast, defined as the difference of the scattering length density (SLD) between the silica matrix and the pore content:

$$I(Q) = A(\rho_{SiO_2} - \rho_p)^2 \tag{1}$$

where A is a constant term,

$$\rho = \sum_i b_i \frac{dN_A}{M_w} \tag{2}$$

ρ is the SLD of a molecule consisting of i atoms (in an empty pore, $\rho_p=0$, while in a pore filled with IL, $\rho_p=\rho_{IL}$), b_i is the coherent neutron scattering length of the individual atoms in the molecule, d is the bulk density of the scattering object, M_w is its molecular weight and N_A is the Avogadro number. The method has previously been utilised for measuring the pore filling of SBA-15 by carbon for the synthesis of ordered nanoporous carbons [45]. Further, it has also been employed for evaluating the density, d, of fluids confined within the pores of ordered mesoporous materials under various pressures and temperatures [46-47] In this work, since the SANS experiment has been carried out under ambient conditions, one would assume that the density of the confined IL will be approximately the same with that of the bulk one. Indeed, XRD results confirmed this argument in the case of samples loaded with IL via physical imbibition, where no evidence for room temperature IL crystallisation under confinement was observed. Following eq 1, when the pores are completely filled with IL, the intensity ratio of the reflections of the pristine to the IL-loaded matrices will be equal to the squared SLD ratio:

$$\frac{\int_{Q_1}^{Q_2} I_{SiO_2-empty\ pore}(Q)Q^2\mathrm{d}Q}{\int_{Q_1}^{Q_2} I_{SiO_2-IL}(Q)Q^2\mathrm{d}Q}=\left(\frac{\rho_{SiO_2}}{\rho_{SiO_2}-\rho_{IL}}\right)^2 \tag{3}$$

where the first term is the calculated integrated intensity ratio, R_I, of the Bragg reflections; the limits of the integrals, Q_1 and Q_2 extend over the tails of the peaks. The diffuse scattering arising from pore correlations was treated as a continuous background [48]. In particular, for the fitting of each peak a linear background was used. Further, the incoherent background has been subtracted from the measured intensities in the case of IL treated samples. The second term, R_{SLD}, can be deduced by calculating the SLD of IL and silica respectively; in the case of IL, according to eq 2, ρ_{IL}=1.6·10^{10} cm^{-2} (d=1.38 g/cm^3 at 20 °C). We should note that this is the value for the IL confined via physical imbibition (MCM_PHYS and SBA_PHYS samples). On the other hand, the SLD of silanised-IL confined by the "grafting to" method (MCM_SILP and SBA_SILP) cannot be estimated because of the presence of the silane part. In this regard, the estimation of the IL skeleton density, *d*, is not possible.

Further, contrast-matching SANS can be employed for the experimental SLD calculation of MCM and SBA samples. The fact that hydrogen and deuterium have scattering lengths of opposite sign means that, neutrons not only can "see" hydrogen isotopes but they can also differentiate between them. It is then possible to match the SLD of the pristine materials (mostly consisted of silica) with an appropriate mixture of water/heavy water. As a result, contrast-matching between the water and the host material can be achieved resulting in the minimisation of the SANS signal ($\rho_p = \rho_{H_2O/D_2O}$ in eq 1). Based on previous contrast-matching SANS measurements performed on these materials [46, 49-54], we used a H_2O/D_2O mixture of 0.40 H_2O volume fraction for both pristine MCM and SBA samples which should "match" the SLD of the silica matrix ($\rho_{SiO_2} \approx 3.6\cdot 10^{10}\,\mathrm{cm}^{-2}$). Indeed, when the samples were immersed in this particular mixture (MCM_w, SBA_w), the Bragg reflections were entirely suppressed and only a constant background remained, mostly due to the incoherent scattering from the protons of H_2O (figures 4a and 4b). In addition, the remaining SANS signal at lower *Q* values (Q<0.2 nm^{-1}), arising mainly from intergrain scattering, was still observed. However, it was much lower (1-2 orders of magnitude) compared to the dry samples. This suggests that an almost complete contrast-matching has been achieved.

In the case of SBA samples (SBA and SBA_PHYS), the value of the integrated intensity ratio of (10) Bragg peaks, R_I=3.6. In comparison with the value of the squared SLD ratio, R_{SLD}=3.35±0.25, one can claim safely a complete pore filling with IL. The result is also in agreement with the nitrogen adsorption measurements, previously discussed. For the MCM samples, however, the peak integrated intensity ratio, R_I =3.0, is lower than R_{SLD}, implying that the pores of MCM_PHYS sample have not been totally filled with IL. The argument is further enhanced by taking into consideration the small nitrogen uptake observed from the adsorption isotherm data. The result can be attributed to the enhanced attractive forces between the confined IL molecules and the pore wall. The degree of pore filling by IL in the MCM_PHYS sample has been further investigated by modeling the SANS data. In this case, eqs 1 and 3 are not longer valid because we are now dealing with a three-phase system consisting of the silica matrix, the IL layer and the empty pore "core". The modulation of the peak intensities before and after the adsorbed IL can be reproduced by calculating the form factor of pores and IL via appropriate density models [55]. In particular, the scattering amplitude of a uniform core-shell cylinder with three density levels i.e. a dense silica matrix, a confined IL layer and an empty pore “core” can be analytically expressed [56]. The application of this model, despite the lack of high-order reflections, fits reasonably with the experimental data for a pore of radius R_p=1.6 nm (in agreement with N_2 adsorption results, table 1) covered with an IL layer having thickness, t=1.4 nm (figure 5). As a result, the pores of MCM_PHYS sample are almost filled with IL and only the pore “core”, having radius R_p-t= 0.2 nm, remains empty.

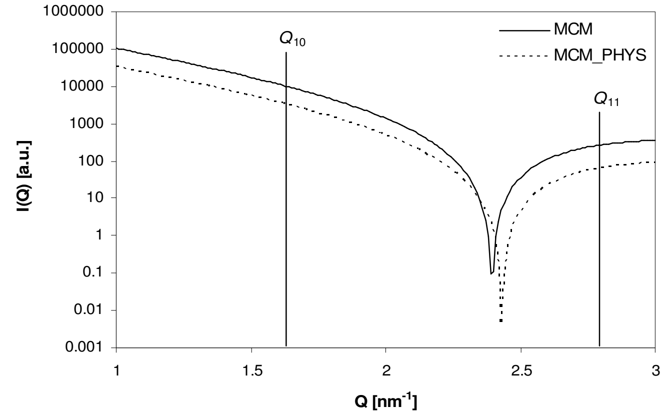

Figure 5. SANS fit for the intensities for the pristine and for loaded with IL via physical imbibition MCM samples for R_p=1.6 nm and t=1.4 nm. The vertical lines denote the positions of the (10) and (11) diffraction peaks.

As previously mentioned, no quantitatively analysis can be performed for the samples treated with the “grafting to” method. However the increased intensity of Bragg peaks for the SBA_SILP sample compared to the MCM_SILP one, suggests a smaller IL loading, in agreement with N_2 porosimetry results. More specific, this intensity increase, especially of the first-order (10) reflection, has also been observed by the performance of *in situ* SANS [40, 47] and SAXS [53, 57] measurements during the initial stages of fluid adsorption on ordered mesoporous MCM-41 and SBA-15 respectively.

As a further step, the pores of the samples treated with IL were filled with the same water mixture that “matches” the silica matrix (MCM_PHYS_w, MCM_SILP_w, SBA_PHYS_w, SBA_SILP_w). In comparison with the dry IL loaded samples, one would not expect significant changes to the SANS signal since their pores are almost (MCM_IL) or completely filled (SBA_IL) with IL. For instance, in a recent study, surfactant adsorption in SBA-15 (with R_p=4 nm) has been studied by SANS [56] The influence of the layer thickness of the adsorbed surfactant films on the scattering curve was investigated by contrast-matching the silica with the appropriate H_2O/D_2O mixture. The calculated thickness of the surfactant films varied between 1 and 3 nm. As the film thickness decreased, a systematic lowering (but not elimination) of the intensities of the Bragg reflections was observed. Our results, however, show clearly that in all (loaded with confined IL) wet samples the peaks are completely vanished, as similarly observed with the pristine contrast-matched samples (figures 4a and 4b). It should be stressed that this behaviour is observed even at physically-loaded samples where the pores are almost (MCM_PHYS) or completely filled (SBA_PHYS) with IL. This is an experimental confirmation of the enhanced solubility of the water in the IL.

Another interesting feature of the pristine and physically-loaded wet samples is that, in the high Q region, the dominated flat incoherent scattering is roughly the same for all samples, except for the pristine one (MCM_w) for which it is higher. This could be attributed to the larger pore volume of MCM compared to that of the SBA (table 1), resulting in a larger amount of adsorbed water and, thus, the presence of more hydrogen atoms. The solubility of the water mixture in IL would not differ between the silica samples (MCM_PHYS and SBA_PHYS respectively), and by taking into consideration that the incoherent background of MCM_PHYS_w is lower than that of the MCM_w and comparable to the correspondent SBA_PHYS_w sample one would possibly suggest that the pore “core” remains empty after the water immersion in the MCM_PHYS sample. As a result, the amount of adsorbed water in both contrast-matched samples loaded with IL via physical imbibition would be roughly the same. Although the size of the “core” diameter (0.4 nm) would allow diffusion of water molecules, the contrast-matching SANS measurements imply that this is not the case. A possible explanation could be that the IL molecules in the adsorbed layer are oriented with the negative ion towards the silica wall and the positive (hydrophobic) towards the pore “core”. This is the reason why there is no water entrance into the empty pore “core”. It is important to note that issues related to the orientation of ILs ions in accordance to the surface charge are very important for their application in electrified interfaces and electrochemical systems. For this reason, many studies both theoretical and experimental have been devoted to explain the distinct capacitance properties of ILs at the electrode surface, in which the cations and anions of the ILs can form an alternate layer [58-61]. However, there are major improvements still needed [62]. Another interesting observation concerning the wet samples prepared by the “grafting to” method is that the incoherent background for SBA_SILP_w is a bit higher than that of MCM_SILP_w. This result also implies that some of the pore “cores” of MCM_SILP would be inaccessible to water molecules resulting in a less amount of adsorbed water. One should mention that the complete blockage of a fraction of MCM’s pores was also concluded from the N_2 adsorption measurements as previously discussed. In this work we have showed that SANS has the potentiality to indirectly predict the ion layers formation of [bmim][PF_6] when confined in mesostructured silicas. Further attempts will be made in the direction to correlate our results with the findings of other advanced electrochemical and AFM methods [63].

4. Conclusions

SANS, contrast-matching SANS, XRD and nitrogen adsorption measurements of IL confined on the pores of ordered mesoporous materials have been presented. IL was introduced by two different methods such as physical imbibition and chemical grafting. In the case of IL confined by physical imbibition both SANS and nitrogen adsorption measurements suggest a complete pore filling with IL for SBA-15, and reveal that only a small fraction of pore volume, the pore “core” is empty for MCM-41. The pore size and the thickness of the IL layer were evaluated by modeling the SANS data. In addition, according to XRD results, there was no evidence for ordering of the confined IL phase. On the other hand, SANS and adsorption measurements suggest a partial pore filling with IL for the chemically grafted SILP samples whereas XRD results indicate a degree of ordering of the grafted IL phase. Moreover, the contrast-matching SANS results from all IL-loaded samples confirm the enhanced solubility of water in IL. They also provide evidence that water does not enter the empty pore “core” of the physically-loaded MCM-41 possibly due to the orientation of IL molecules in the adsorbed layer. Finally, in the case of samples prepared by the “grafting to” method both the adsorption and contrast-matching SANS experiments suggest a complete blockage of a fraction of MCM’s pores by the silylated IL resulting in the inaccessibility of both nitrogen and water molecules towards the pore “cores”.

Acknowledgements

This research project has been supported by the European Commission under the 7th Framework Programme through the Key Action: Strengthening the European Research Area, Research Infrastructures. Contract n°: 226507 (NMI3).

References

[1] Chen, S, Kobayashi K, Miyata Y, Imazu N, Saito T, Kitaura R and Shinohara H. 2009 *J. Am. Chem. Soc.* **131** 14850

[2] Millefiorini S, Tkaczyk A H, Sedev R, Efthimiadis J and Ralston J 2006 *J Am. Chem. Soc.* **128** 3098

[3] Gao L and McCarthy T J 2007 *J. Am. Chem. Soc.* **129** 3804
[4] Wang J and Li Y J 2009 *J. Am. Chem. Soc.* **131** 5364
[5] Ramsay J D F 1998 *Adv. Coll. Inter. Sci.* **76-77** 13
[6] Mitropoulos A C, Kanellopoulos N K, Stefanopoulos K L and Heenan, R K 1998 *J. Coll. Inter. Sci.* **203** 229
[7] Makri P K, Stefanopoulos K L, Mitropoulos A C, Kanellopoulos N K and Treimer W 2000 *Physica* B **276-278** 477
[8] Hoinkis E, Lima E B and Schubert-Bischoff P 2004 *Langmuir* **20** 8823
[9] Stuhrmann H B and Miller A. 1978 *J. Appl. Cryst.* **11** 325
[10] Charalambopoulou G C, Steriotis T A, Hauss T, Stefanopoulos K L and Stubos A K 2002 *Appl. Phys.* A **74** S1245
[11] Steriotis T A, Stefanopoulos K L, Keiderling U, De Stefanis A and Tomlinson A A G 2002 *Chem. Commun.* **20** 2396
[12] Calo J M and Hall P J 2004 *Carbon* **42** 1299
[13] Lelong G, Price D L, Brady J W and Saboungi M L 2007 *J Chem. Phys.* **127** 065102
[14] Mitropoulos A C, Stefanopoulos K L and Kanellopoulos N K 1998 *Microporous Mesoporous Mater.* **24** 29
[15] Katsaros F K, Steriotis T A, Stefanopoulos K L, Kanellopoulos N K, Mitropoulos A C, Meissner M and Hoser A 2000 *Physica* B **276-278** 901
[16] Steriotis T A, Stefanopoulos K L, Mitropoulos A C, Kanellopoulos N K, Hoser A and Hofmann M 2002 *Appl. Phys.* A **74** S1133
[17] Steriotis T A, Stefanopoulos K L, Kanellopoulos N K, Mitropoulos A C and Hoser A 2004 *Colloids Surf.* A **1-3** 239
[18] Eschricht N, Hoinkis E and Mädler F 2007 *Langmuir* **23** 2145
[19] Sel O, Brandt A, Wallacher D, Thommes M and Smarsly B 2007 *Langmuir* **23** 4724
[20] Mascotto S, Wallacher D, Kuschel A, Polarz S, Zickler G A, Timmann A and Smarsly B M 2010 *Langmuir* **26** 6583
[21] Kikkinides E S, Stefanopoulos K L, Steriotis T A, Mitropoulos A C, Kanellopoulos N K and Treimer W 2002 *Appl. Phys.* A **74** S954
[22] Eschricht N, Hoinkis E, Mädler F, Schubert-Bischoff P and Röhl-Kuhn B 2005 *J. Coll. Inter. Sci.* **291** 201
[23] Eastoe J, Gold S, Rogers S E, Paul A, Welton T, Heenan R K and Grillo I. 2005 *J. Am. Chem. Soc.* **127** 7302
[24] Tasserit C, Koutsioubas A, Lairez D, Zalczer G and Clochard M-C 2010 *Phys. Rev. Lett.* **105** 260602
[25] Kresge C T, Leonowicz M E, Roth W J, Vartuli J C and Beck J S 1992 *Nature* **359** 710
[26] Zhao D, Feng J, Huo Q, Melosh N, Fredrickson G H, Chmelka B F and Stucky G D 1998 *Science* **279** 548
[27] Romanos G E, Vangeli O C, Stefanopoulos K L, Kouvelos E P, Papageorgiou S K, Favvas E P and Kanellopoulos N K 2009 *Microporous Mesoporous Mater.* **120** 53
[28] Vangeli O C, Romanos G E, Beltsios K G, Fokas D, Kouvelos E P, Stefanopoulos K L and Kanellopoulos N K 2010 *J. Phys. Chem.* B **114** 6480
[29] Barret E P, Joyner L G and Halenda P H 1951 *J. Am. Chem. Soc.* **73** 373
[30] Tarazona P 1985 *Phys. Rev.* A **31** 2672
[31] Neimark A V, Ravikovitch P I and Vishnyakov A 2003 *J. Phys: Conden. Matter* **15** 347
[32] Mergia K, Stefanopoulos K L, Ordás N and García-Rosales C *2010 Microporous Mesoporous Mater.* **134** 141
[33] Brûlet A, Lairez D, Lapp A and Cotton J-P 2007 *J. Appl. Cryst.* **40** 165
[34] Brunauer S, Emmet P H and Teller E J 1939 *J. Am. Chem. Soc.* **60** 309
[35] Sing K S W, Everett D H, Haul R A W, Moscou L, Pierotti R A, Rouquérol J and Siemieniewska T 1998 *Pure Appl. Chem.* **57** 603

[36] Cregg S J and Sing K S W 1982 *Adsorption, Surface Area and Porosity* (New York: Academic Press)
[37] Singh M P, Singh R K and Chandra S, 2011 *J. Phys. Chem.* B **115** 7505
[38] Chen S, Wu G, Sha M and Huang S 2007 *J Am. Chem. Soc.* **129** 2416
[39] Porod G 1951 *Kolloid Z.* **124** 83
[40] Ramsay J D F, Kallus S and Hoinkis E 2000 *Stud. Surf. Sci. Catal.* **128** 439
[41] Kallus S, Hahn A and Ramsay J D F 2003 *Eur. Phys. J.* E **12** S31
[42] Liu D, Zhang Y, Chen C-G, Mou C-Y, Poole P H and Chen S-H 2007 *Proc. Nat. Acad. Sci.* **104** 9570
[43] Edler K J, Reynolds P A and White J W 1998 *J. Phys. Chem.* **102** 3676
[44] Ramsay J D F and Hoinkis E 1998 *Physica* B **248** 322
[45] Ehrburger-Dolle F, Morfin I, Geissler E, Bley F, Livet F, Vix-Guterl C, Saadallah S, Parmentier J, Reda M, Patarin J, Iliescu M and Werckmann J 2003 *Langmuir* **19** 4303
[46] Morineau D, Guégan R, Xia Y and Alba-Simionesco C 2002 *J. Chem. Phys.* **117** 8966
[47] Steriotis T A, Stefanopoulos K L, Katsaros F K, Gläser R, Hannon A C and Ramsay J D F 2008 *Phys. Rev.* B **78** 115424
[48] Zickler G A, Jähnert S, Wagermaier W, Funari S S, Findenegg G H and Paris O 2006 *Phys. Rev.* B **73** 184109
[49] Glinka C J, Nicol J M, Stucky G D, Margolese D, Huo Q, Higgins J B and Leonowicz M E 1996 *J. Porous Mater.* **3** 93
[50] Tun Z, Mason P C, Mansour F K and Peemoeller H 2002 *Langmuir* **18** 975
[51] Erko M, Wallacher D, Brandt A and Paris O 2010 *J. Appl. Cryst.* **43** 1
[52] Müter D, Shin T, Demé B, Fratzl P, Paris O and Findenegg G H 2010 *J Phys. Chem. Lett.* **1** 1442
[53] Schreiber A, Ketelsen I, Findenegg G H and Hoinkis E 2007 *Stud. Surf. Sci. Catal.* **160** 17
[54] Linton P, Rennie A R and Alfredsson V 2011 *Solid State Sci.* **13** 793
[55] Impéror-Clerc M, Davidson P and Davidson A 2000 *J. Am. Chem. Soc.* **122** 11925
[56] Shin T, Findenegg G H and Brandt A 2006 *Prog. Colloid Polym. Sci.* **133** 116
[57] Jähnert S, Müter D, Prass J, Zickler G A, Paris O and Findenegg G H 2009 *J. Phys. Chem.* C **113** 15201
[58] Maolin S, Guozhong W, Qiang D, Zhongfeng T and Haiping F 2010 *Langmuir* **26** 12667
[59] Pinilla C, Del Pópolo M G, Kohanoff J and Lynden-Bell R M 2007 *J. Phys. Chem.* B **111** 4877
[60] Buzzeo M C, Evans R G and Compton R G 2004 *Chem. Phys. Chem.* **5** 1106
[61] Baldelli S. 2005 *J. Phys. Chem.* B **109** 13049
[62] Kornyshev A A 2007 *J. Phys. Chem.* B **111** 5545
[63] Atkin R and Warr G G 2007 *J. Phys. Chem.* C **111** 5162